Quantifying Uncertainty Due to Climate Variability in Vehicle-Integrated Photovoltaic Yield Predictions

Timofey Golubev
ThermoAnalytics, Inc., Calumet, MI, 49913, USA

***Abstract*—This work uses a surrogate modeling approach to quantify the uncertainty due to climate variability in vehicle-integrated photovoltaic (VIPV) energy yield predictions. An artificial neural network (ANN) is trained to predict VIPV yield from weather data using results from thermal-electrical simulations of a VIPV system. The ANN is then used with 23 years of historical weather data to evaluate the variability of the VIPV system's yield at 260 locations in North America.**

***Index Terms*—vehicle-integrated photovoltaics, uncertainty quantification, energy yield, surrogate modeling, artificial neural network, electric vehicles, thermal-electrical**

I. Introduction

The rapid development of electric vehicles combined with increasing efficiencies and reducing costs of photovoltaic cells has resulted in increased interest in vehicle-integrated photovoltaics (VIPVs) [1], [2]. Climate conditions can have a significant impact on VIPV system energy production [3]. Therefore, evaluating VIPVs through simulation is necessary to predict VIPV yield under a wide range of environmental conditions. However, detailed physics-based VIPV models that calculate the incident irradiance on curved surfaces and consider thermal effects are computationally expensive, making them impractical to use directly for comprehensive studies. To address this limitation, we developed an approach for training a surrogate model on physics-based simulations for rapid prediction of VIPV energy yields [4]. In this work we use our surrogate modeling approach to quantify uncertainty due to climate variability in VIPV yield predictions for 260 locations in North America.

II. Methodology

A. Surrogate Model

We train an artificial neural network (ANN) to predict VIPV yield using results from a coupled thermal-electrical model of a vehicle with on-board PVs and the surrogate modeling approach developed in our previous work [4]. We briefly summarize the surrogate modeling approach in this section. The thermal-electrical model was created in the commercial heat transfer software TAITherm [5], which uses a numerical, finite volume method based on first principles physics to solve for heat transfer due to conduction, convection, and radiation. A PV equivalent circuit electrical model was implemented in Python and coupled with the thermal model. To simulate the climatic conditions, we applied typical meteorological year (TMY) weather data from the National Solar Radiation Database (NSRDB) [6] as boundary conditions. As an example model, we simulated the VIPV energy production from 2.8 m^2 of SunPower Maxeon Gen III solar cells integrated into the roof of a sports utility vehicle. Equivalent circuit parameters for the solar cells were derived from the manufacturer datasheet [7] and are listed in our previous work [4].

To generate the training dataset for the surrogate model creation, we ran year-long thermal-electrical simulations of the VIPV system with hourly time-steps. We use the following model inputs (i.e. features): global horizontal irradiance (GHI), direct normal irradiance (DNI), direct horizontal irradiance (DHI), solar azimuth, solar zenith, and ambient air temperature. The target variable is the power output of the VIPV in each hour of the year. For the surrogate model, we use the best performing model architecture from our previous work, a multi-layer perceptron neural network from the Scikit-Learn Python package (version 0.24.2) [8] with a logistic activation function, 3 hidden layers with 100 neurons in each, an L2 penalty parameter of 10^{-5}, and the `lbfgs` solver with 5000 maximum iterations. In our previous work, we trained the surrogate models using a single year-long TAITherm simulation of the VIPV system in Seattle, Washington. In this work, we retrained the ANN using TAITherm results from two locations instead of one: Seattle, Washington and Phoenix, Arizona. The second location was added to improve the model accuracy for predictions at new locations by providing the ANN with training data that includes a wider range of climate conditions. After training, we tested the ANN's performance by comparing its predictions to TAITherm results for six additional locations in the United States.

B. Sensitivity Analysis

To evaluate the sensitivity of the VIPV yield prediction on the model inputs, we performed a Saltelli sensitivity analysis with the OpenTURNS Python package [9]. Historical weather data from multiple locations in the U.S. was used to estimate non-parametric probability distributions of the inputs. These input distributions were then sampled 80,000 times and Sobol indices [10], which quantify the sensitivity of the VIPV yield to each model input, were calculated.

C. Uncertainty Quantification

We used the ANN and historical weather data from the NSRDB (PSMV3 dataset for 1998-2020) to quantify the variability in annual VIPV yield at 260 locations in or near the United States. The ANN model was run to predict the hourly VIPV energy production for each of the 5980 years (260 locations x 23 years) of weather data. The ANN model

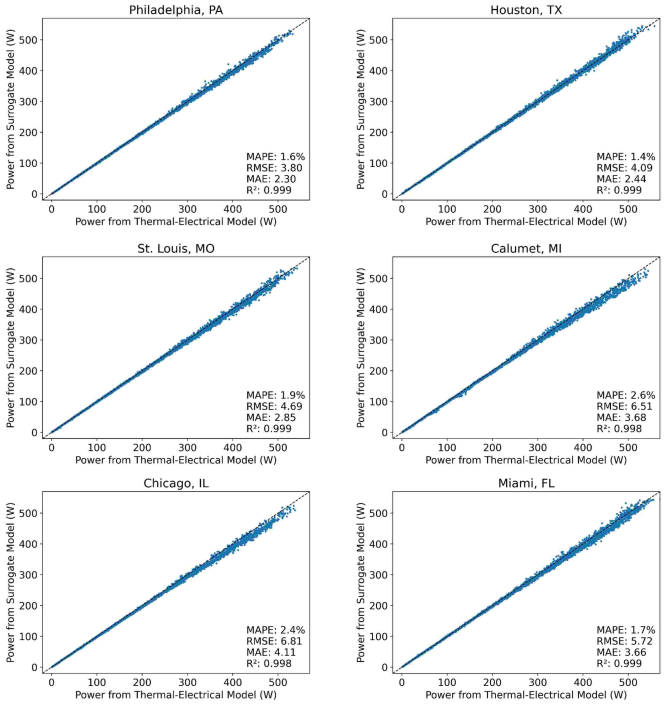

Fig. 1. Comparison of the VIPV power output prediction from the surrogate model versus the thermal-electrical model for six test locations.

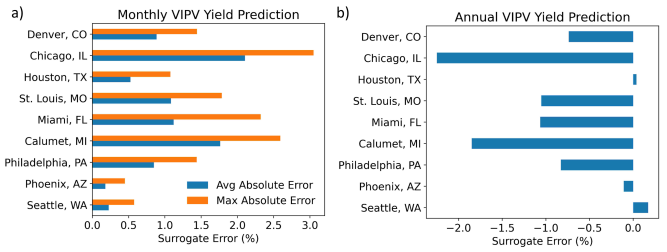

Fig. 2. Surrogate model's deviation from thermal-electrical model results for monthly and annual total VIPV yield predictions.

evaluation took only 0.18 seconds per year (on an Intel i9-10900K). The hourly predictions were then summed for each year at each location. The variability in annual VIPV yield at each location was quantified by the percent difference between the median annual yield and the P90 annual yield (i.e. yield that was predicted to be exceeded in 90% of the historical years) [11].

III. Results and Discussion

A. Surrogate Model Validation

Fig. 1 shows comparisons of the hourly PV power output prediction from the ANN and the thermal-electrical model on the test locations. The mean absolute error (MAE), root mean square error (RMSE), mean absolute percent error (MAPE), and coefficient of determination (R^2) were used to quantify model performance. The surrogate model's hourly power output predictions are on average within 1.4-2.6% (depending on location) of the thermal-electrical model results, indicating

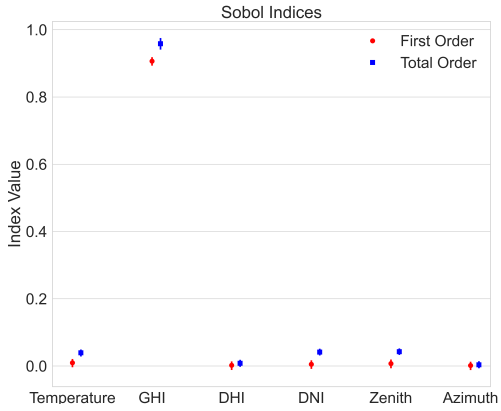

Fig. 3. Sobol sensitivity indices.

good prediction accuracy. Fig. 2 displays the error between the surrogate and thermal-electrical models' total monthly and annual VIPV yield predictions. We find that the ANN has good prediction accuracy for the monthly and annual total yields with predictions within 3% of the thermal-electrical results. These results validate that the surrogate model is able to replicate the full thermal-electrical model's predictions with sufficient accuracy to be used for sensitivity analysis and uncertainty quantification.

B. Sensitivity Analysis

Fig. 3 quantifies the sensitivity of the model to its input parameters in terms of Sobol indices where parameters with larger index values correspond to a greater sensitivity to that parameter. As expected, the VIPV energy production is most sensitive to the GHI. The VIPV yield also has smaller non-zero sensitivity to air temperature, DNI, and zenith angle. The first order indices for temperature, DNI, and zenith angle are near zero while the total order are non-zero indicating that the VIPV yield depends on combinations of these parameters, instead of directly on each parameter individually.

C. Uncertainty Quantification

As an example of the interannual yield distributions at individual locations, Fig. 4 shows the distributions of predicted VIPV yield in 10 locations from 2001-2020 and Fig. 5 shows the monthly yields for four of these locations. We see that there can be significant variability in both annual and monthly energy production from year to year. In Fig. 5, three of the four locations exhibit strong seasonality in VIPV yield with summer energy production being several times greater than winter production. Calumet, MI, the northernmost location of these four, exhibits the strongest seasonality with summer yields approaching those of locations much further south such as St. Louis and Miami, while winter yields are very low. Miami, the southernmost location of the four, has the least seasonality.

Fig. 6a shows the medians of the predicted annual VIPV yields from 1998-2020 for 260 locations. The median VIPV annual yield has similar trends to the annual solar GHI at these

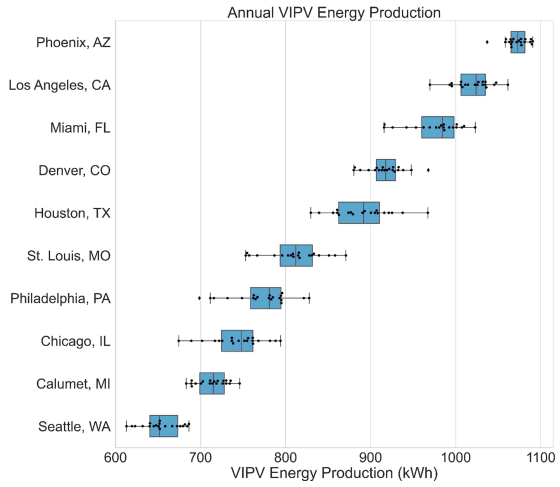

Fig. 4. Uncertainty quantification of annual VIPV yield in ten locations using historical weather data from 2001-2020.

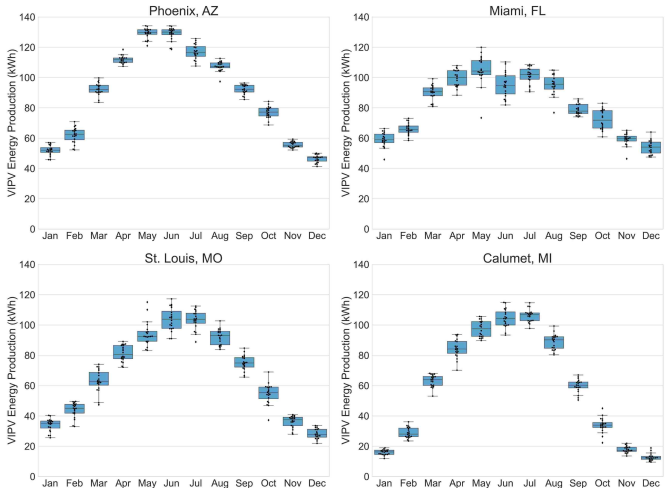

Fig. 5. Uncertainty quantification of monthly VIPV yield in four locations using historical weather data from 2001-2020.

locations with the highest annual yields being in the southwest of the region studied and the lowest yields being in the north [6]. Fig. 6b shows the variability in predicted annual VIPV yields in terms of the percent difference between the P90 and median (P50) values for each location. The U.S. Southwest and portions of Wyoming and Montana (just east of the Rocky Mountains) are predicted to have the least variability in VIPV energy yield with interannual fluctuations expected to be only 1-3% from the median. Locations in the U.S. Southeast, Mid-Atlantic, and Northwest Coast are predicted to have in-general the greatest variability in yield with fluctuations of 5-8.4%. The median of the annual variabilities for all locations is 4.1%.

We also calculated the uncertainty due to interannual climate variability in monthly VIPV yields for all locations. Fig. 7 presents a statistical summary of the results. In general, the uncertainty is highest in the winter months and lowest in the summer months. The winter months have the largest range of values for uncertainties in different locations, with some

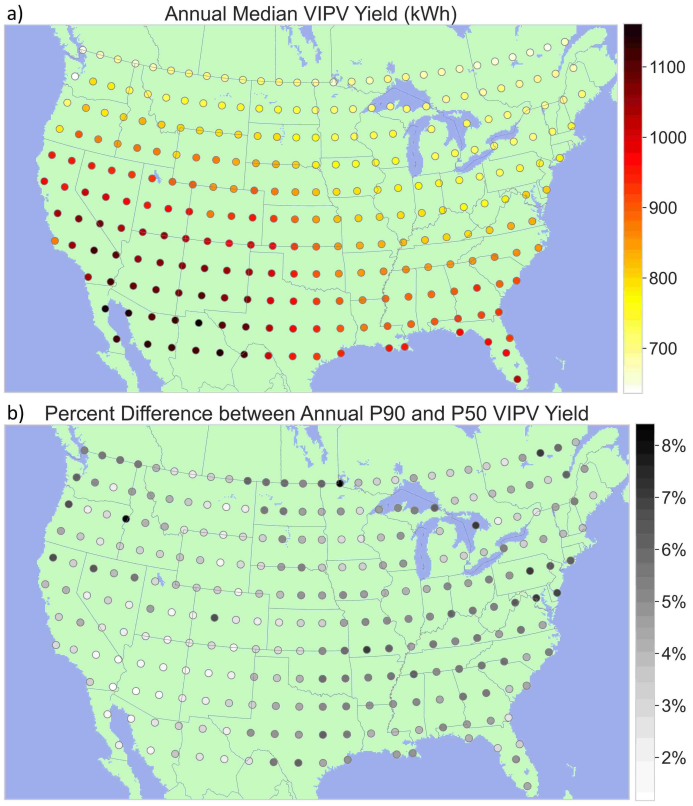

Fig. 6. Summary of VIPV yield predictions for 1998-2020. a) Median annual VIPV yields. b) Interannual variability of VIPV yields quantified as percent difference between P90 and median (P50) values.

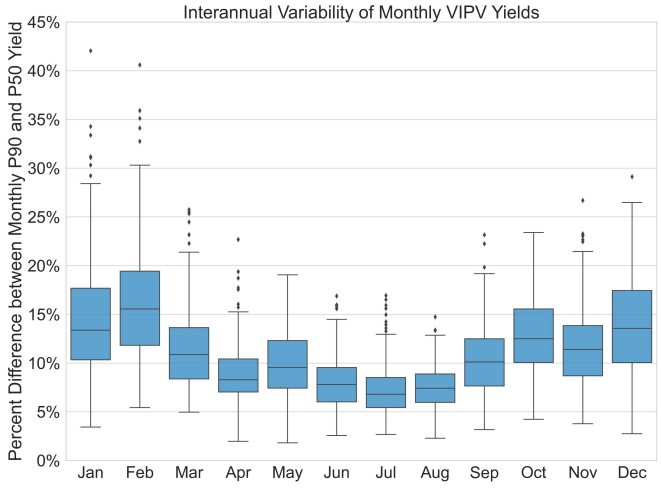

Fig. 7. Statistical summary of interannual variability of monthly total VIPV yields for all 260 locations quantified as percent difference between P90 and median (P50) values for each location.

outlier locations having greater than 30% difference between P90 and P50 values in January and February.

Fig. 8 shows a summary of the medians of the monthly VIPV yields for 1998-2020 for the 260 locations considered in this study. The trends are consistent with monthly trends in

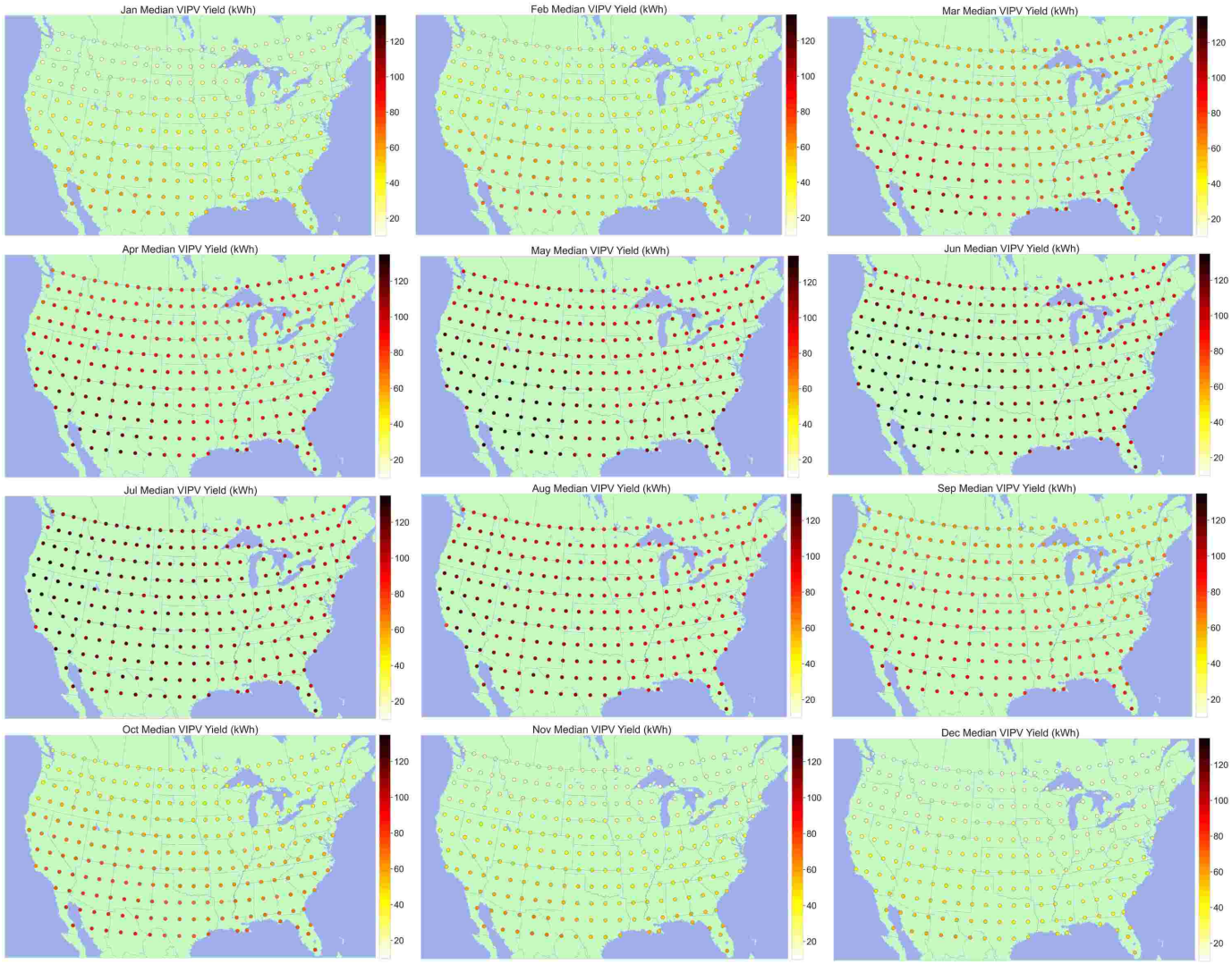

Fig. 8. Summary of median monthly VIPV yields predicted for 1998-2020.

the GHI for each location. Like seen with the annual median yields, the highest yields during any given month tend to be in the southwest of the region studied, while the lowest yields are in the north.

Fig. 9 shows the variability in predicted monthly VIPV yields. Overall, the variability in monthly yields is significantly larger in the winter months than in the summer months. The southwest is predicted to have the lowest variabilities in the winter months. In the summer months, the yield variabilities of the majority of locations are reduced and the variabilities are more similar throughout the entire region.

IV. Conclusion

This work uses an ANN surrogate model, which was trained on physics-based thermal-electrical simulations, to quantify uncertainty due to climate variability in VIPV energy yield predictions. The high computational efficiency of the surrogate model improves the practicality of performing uncertainty quantification, which often requires thousands of model runs. The ANN was found to have less than 3% error in hourly, monthly total, and yearly total yield predictions when compared to the physics-based simulations, thus validating that it can be used reliably for uncertainty quantification. A sensitivity analysis showed that the uncertainty in VIPV yield is most sensitive to GHI with smaller non-zero sensitivities due to the combined effects of temperature, DNI, zenith angle, and GHI. The ANN was applied to predict the expected variability in VIPV energy production at 260 locations in North America. Areas with generally lower or higher interannual variability were identified. Interannual variability of total monthly yields of four locations were evaluated as a demonstration of the impact of geographic location on VIPV yield and its uncertainty. In future work, the surrogate VIPV model could be combined with electric vehicle energy consumption simulations to predict the solar-powered driving range in different locations.

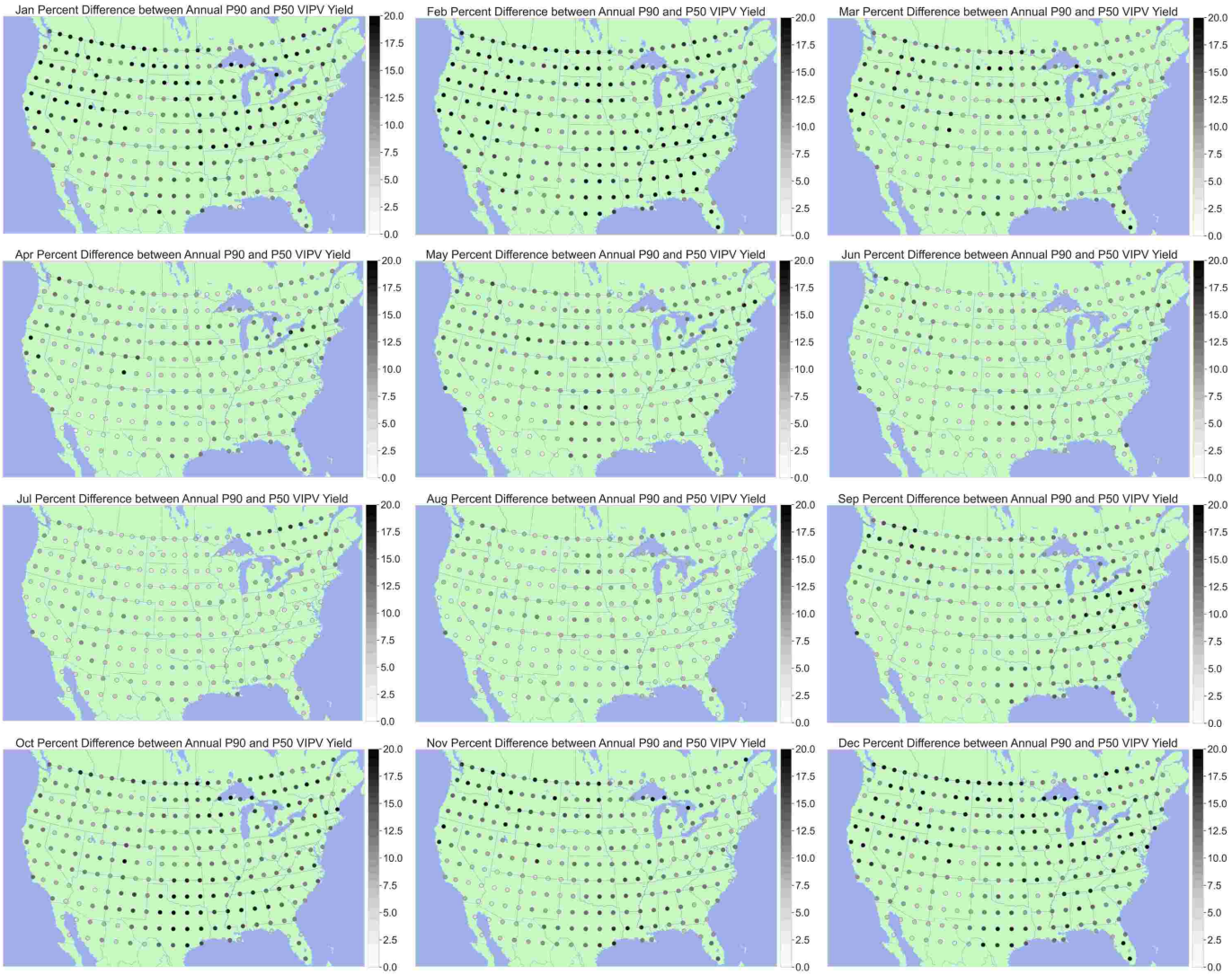

Fig. 9. Summary of interannual variability of monthly VIPV yields predicted for 1998-2020.

REFERENCES

[1] B. Commault, T. Duigou, V. Maneval, J. Gaume, F. Chabuel, E. Voroshazi, "Overview and perspectives for vehicle-integrated photovoltaics," *Appl. Sci.*, vol. 11, 2021, doi:10.3390/app112411598.

[2] M. Heinrich et al., "Potential and challenges of vehicle integrated photovoltaics for passenger cars," in 37th European PV Solar Energy Conference and Exhibition (EU PVSEC), 2020.

[3] C. Thiel et al., "Impact of climatic conditions on prospects for integrated photovoltaics in electric vehicles," *Renew. Sustain. Energy Rev.*, vol. 158, 2022, doi:10.1016/j.rser.2022.112109.

[4] T. Golubev, "Surrogate modeling for rapid prediction of energy yield from vehicle-integrated photovoltaics," in *49th IEEE Photovoltaic Specialists Conference*, 2022, doi:10.1109/PVSC48317.2022.9938713.

[5] *TAITherm* (2022.2.0). ThermoAnalytics, Inc.

[6] M. Sengupta, Y. Xie, A. Lopez, A. Habte, G. Maclaurin, and J. Shelby, "The national solar radiation database (NSRDB)," *Renew. Sustain. Energy Rev.*, vol. 89, pp. 51–60, 2018, doi:10.1016/j.rser.2018.03.003.

[7] Sunpower. "Maxeon 3 BLK". [Online]. Available: https://sunpower.maxeon.com/int/sites/default/files/2020-09/sp_mst_MAX3-375BLK_355BLK_ds_en_a4_mc4_532497.pdf [Accessed: 21-Nov-2021].

[8] F. Pedregosa et al., "Scikit-learn: Machine learning in python," *J Mach Learn Res.*, vol. 12, pp. 2825–2830, 2011.

[9] M. Baudin, A. Dutfoy, B. Iooss, A. Popelin, "OpenTURNS: An industrial software for uncertainty quantification in simulation," *Handbook of Uncertainty Quantification*, 2017, doi: 10.1007/978-3-319-12385-1_64.

[10] I. M. Sobol, "Global sensitivity indices for nonlinear mathematical models and their Monte Carlo estimates," *Mathematics and Computers in Simulation*, vol. 55, pp. 271-280, 2001, doi:10.1016/S0378-4754(00)00270-6.

[11] D. Ryberg, J. Freeman, N. Blair, "Quantifying interannual variability for photovoltaic systems in PV Watts," NREL Technical Report, 2015, doi:10.2172/1226165.